Optical Materials 31 (2009) 1000–1006

Contents lists available at ScienceDirect

Optical Materials

journal homepage: www.elsevier.com/locate/optmat

Third-order nonlinear optical susceptibilities of new copolymers containing alternate 3,4-dialkoxythiophene and (1,3,4-oxadiazolyl)pyridine moieties

Pramod Kumar Hegde [a], A. Vasudeva Adhikari [a,*], M.G. Manjunatha [a], P. Poornesh [b], G. Umesh [b]

[a] Organic Chemistry Division, Department of Chemistry, National Institute of Technology Karnataka, Surathkal, Mangalore-575025, India
[b] Department of Physics, National Institute of Technology Karnataka, Surathkal, Mangalore-575025, India

ARTICLE INFO

Article history:
Received 30 August 2008
Received in revised form 1 November 2008
Accepted 19 November 2008
Available online 8 January 2009

PACS:
42.70.J
42.70.M
42.70.N

Keywords:
Conjugative polymers
3,4-Dialkoxythiophene
1,3,4-Oxadiazole
Pyridine
NLO properties
Z-scan

ABSTRACT

A new series of conjugated copolymers (**P1**–**P3**) consisting of alternate 3,4-dialkoxythiophene and (1,3,4-oxadiazolyl)pyridine moieties have been synthesized using the precursor polyhydrazide route. They have been characterized by FTIR, ^{1}H NMR spectral and elemental analyses. These copolymers possess well defined structure and exhibit good thermal stability with the onset decomposition temperature in nitrogen at around 300 °C. Their molecular weights were determined by gel permeation chromatography (GPC). The optical and charge-transporting properties of the copolymers were investigated by UV–visible spectroscopy, fluorescence emission spectroscopy and cyclic voltammetry. Their UV–visible absorption spectra showed a λ_{max} at around 342 nm and displayed bluish-green fluorescence in solution state. The band gaps were found to be at about 2.55 eV for all the copolymers. The third-order nonlinear optical properties (NLO) of these copolymers were studied by *Z*-scan technique. The measurements were performed at 532 nm with 7 ns laser pulses using a Nd:YAG laser in solution form. The real part of $\chi^{(3)}$ were estimated to be -0.881×10^{-12}, -0.901×10^{-12} and -1.030×10^{-12} esu for **P1**, **P2** and **P3** respectively. The imaginary part of $\chi^{(3)}$ for the copolymers **P1**, **P2** and **P3** were determined to be 0.192×10^{-12}, 0.253×10^{-12} and 0.272×10^{-12} esu respectively. The copolymers exhibit strong reverse saturable absorption and good optical limiting behaviour at 532 nm.

1. Introduction

Conjugative polymers have been the materials of interest for many researchers in the field of photonics and optoelectronics in the past several years due to their large third-order nonlinear response and related device application [1–3]. A strong delocalization of π-electrons along the polymer chain is known to be the reason for their third-order nonlinearity. These polymers offer good flexibility at both the molecular and bulk levels for the structural modifications that are necessary to optimize them for the practical use [4]. Various conjugated polymers, such as polyacetylene, polydiacetylene, and poly(*p*-phenylene vinylene), have been studied extensively, and large values of third-order nonlinear optical susceptibility $\chi^{(3)}$ have been measured [4,5]. However, the application of these may face the problems in the areas of processing or environmental stability; as a result a number of other conjugated polymers have also been investigated for their third-order NLO properties.

Amongst the various polymers studied, polythiophenes are gaining considerable interest as materials for nonlinear optics because of their large third-order nonlinear response, chemical stability, and processability with suitable substituents [6,7]. Also, good film forming properties, solubility, and adequate mechanical properties made them better choice for device fabrication in comparison with their inorganic counterparts. The good NLO response of these polymers is primarily determined by their molecular structure; hence one can employ molecular modelling to design new structures by introducing suitable substituents. As described by Fuks-Janczarek et al. [8], dipole moment of polythiophene plays an important role in the behavior of their observed UV–vis spectra. Based on theoretical molecular geometry and quantum chemical calculations, they observed that the first absorption maxima shows red shift during changing the number of dimers from $n = 1$ to 15. The shift of the absorption spectra may reflect a specific geometry of the thiophene group and hence affect the optical linearity and nonlinear susceptibilities. By considering all these aspects, few copolymers derived from thiophenes were synthesized and studied for third NLO properties [9–11]. According to authors, donor and acceptor groups along the polymer backbone would be a promising molecular design for enhancing the third-order NLO properties.

In this context, it has been planned to incorporate additional electron withdrawing moiety in between 3,4-dialkoxy substituted thiophenyl oxadiazole systems in our synthetic design of new

* Corresponding author. Tel.: +91 8242474046; fax: +91 8242474033.
E-mail addresses: avchem@nitk.ac.in, avadhikari123@yahoo.co.in (A.V. Adhikari).

0925-3467/$ - see front matter © 2008 Elsevier B.V. All rights reserved.
doi:10.1016/j.optmat.2008.11.015

molecules, in order to enhance electron accepting nature within the polymer chain. It is hoped that the resulting molecules would exhibit better NLO properties. In this report, we describe the synthesis and characterization of a new series of donor-acceptor type of copolymers containing 3,4-dialkoxythiophene as electron rich segment, and 1,3,4-oxadiazole and pyridine moieties as electron deficient units. The third-order nonlinear optical susceptibility of these copolymers was determined using single beam *Z*-scan technique with Nd:YAG nanosecond laser pulses at 532 nm. The copolymers displayed high values of n_2 and $\chi^{(3)}$ and showed strong reverse saturable absorption. These copolymers exhibit good optical power limiting property for nanosecond laser pulses. Further, the concentration dependence of NLO parameters is also reported.

2. Experimental

2.1. Materials and instrumentation

3,4-Dialkoxythiophene-2,5-dicarbohydazides **1a–c** were synthesized from corresponding diethyl 3,4-dialkoxythiophene-2,5-dicarboxylates according to the reported procedure [12]. Dimethylformamide (DMF) and acetonitrile (ACN), dried over CaH_2 were used. Thiodiglycolic acid, diethyl oxalate and tetrabutylammoniumperchlorate (TBAPC) were purchased from Lanchaster (UK). Pyridine-2,6-dicarbonyl chloride and *n*-bromoalkanes were purchased from Aldrich and used as received. All the solvents and reagents were of analytical grade, purchased commercially and used without further purification.

Infrared spectra of all intermediate compounds and polymers were recorded on a Nicolet Avatar 5700 FTIR (Thermo Electron Corporation). The UV–visible and fluorescence spectra were taken in GBC Cintra 101 UV–visible and Perkin Elmer LS55 fluorescence spectrophotometers respectively. ^{1} H NMR spectra were obtained with AMX-400 MHz FT-NMR spectrometer using TMS/solvent signal as internal reference. Elemental analyses were performed on a Flash EA1112 CHNS analyzer (Thermo Electron Corporation). Mass spectra were recorded on a Jeol SX-102 (FAB) Mass Spectrometer. The electrochemical studies of the polymers were carried out using a AUTOLAB PGSTAT30 electrochemical analyzer. Cyclic voltammograms were recorded using a three-electrode cell system, with glassy carbon button as working electrode, a platinum wire as counter electrode and an Ag/AgCl electrode as the reference electrode. Molecular weights of the polymers were determined with a WATERs make Gel Permeation Chromatograph (GPC) against polystyrene standards with teterhydrofuran (THF) as an eluent. The third-order NLO properties of these polymers were studied at 532 nm in DMF solution with 7 ns pulses from a Nd:YAG laser using *Z*-scan technique.

2.2. General procedure for the synthesis of polyhydrazides, *3a–c*

To a mixture of 1 equivalent of appropriate dihydrazides (**1a–c**), 2 equivalents of anhydrous aluminum chloride and 0.1 mL of pyridine, 1 equivalent of diacid chloride (**2**) was added slowly at room temperature with stirring and stirring was continued for 5 h. Further, it was heated at 80 °C for 20 h. After cooling to room temperature the reaction mixture was poured into ice cold water and the precipitate separated was collected by filtration. It was washed with water followed by acetone and finally dried in vacuum to get the corresponding polyhydrazides **3a–c** in 75–85% yield.

3a: Yield: 80%, IR (KBr, *v*): 3320 cm^{-1} (–N–H), 1718 cm^{-1} (>C=O), Elemental: Calcd for ($C_{19}H_{21}N_5O_6S$): C, 51.00%; H, 4.73%; N, 15.65%; S, 7.17%; Found: C, 51.24%; H, 4.55%; N, 15.43%; S, 7.30%.

3b: Yield: 83%, IR (KBr, *v*): 3318 cm^{-1} (–N–H), 1722 cm^{-1} (>C=O), Elemental: Calcd for ($C_{23}H_{29}N_5O_6S$): C, 54.86%; H, 5.80%; N, 13.91%; S, 6.37%; Found: C, 54.70%; H, 5.61%; N, 14.10%; S, 6.20%.

3c: Yield: 85%, IR (KBr, *v*): 3320 cm^{-1} (–N–H), 1715 cm^{-1} (>C=O), Elemental: Calcd for ($C_{27}H_{37}N_5O_6S$): C, 57.94%; H, 6.66%; N, 12.51%; S, 5.73%; Found: C, 57.78%; H, 6.85%; N, 12.33%; S, 5.58%.

2.3. General procedure for the synthesis of polyoxadiazoles, *P1–P3*

A mixture of polyhydrazide (0.5 g) and 20 mL phosphorus oxychloride was heated at 100 °C for 4 h with stirring. The reaction mixture was then cooled to room temperature and poured to excess of ice cold water. The resulting precipitate was collected by filtration, washed with water followed by acetone and dried in vacuum oven to get the copolymers **P1–P3** in 80–85% yield.

P1: Yield: 85%, IR (KBr, *v*): 2920, 2848, 2760, 1583, 1467, 1060 cm^{-1}. Elemental: Calcd for ($C_{19}H_{17}N_5O_4S$): C, 55.47%; H, 4.16%; N, 17.02%; S, 7.79%, Found: C, 55.60%; H, 4.00%; N, 17.22%; S, 7.48%. ^{1}H NMR: ($CDCl_3$, δ, ppm): 0.87 (t, 6H, $-CH_3$), 1.24 (m, 4H, $-CH_2$), 4.34 (t, 4H, $-OCH_2-$), 8.10–8.33 (m, 3H, pyridine). Weight average molecular weight: 8148.

P2: Yield: 80%, IR (KBr, *v*): 2912, 2850, 2758, 1588, 1460, 1060 cm^{-1}. Elemental: Calcd for ($C_{23}H_{25}N_5O_4S$): C, 59.08%; H, 5.39%; N, 14.98%; S, 6.86%, Found: C, 58.81%; H, 5.20%; N, 14.78%; S, 6.50%. ^{1}H NMR: ($CDCl_3$, δ, ppm): 0.88 (t 6H, $-CH_3$), 1.22–1.40(m, 12H, alkyl), 4.32 (t, 4H, $-OCH_2-$), 8.08–8.34 (m, 3H, pyridine). Weight average molecular weight: 9232.

P3: Yield: 84%, IR (KBr, *v*): 2930, 2850, 2765, 1590, 1455, 1060 cm^{-1}. Elemental: Calcd for ($C_{27}H_{33}N_5O_4S$): C, 61.93%; H, 6.35%; N, 13.37%; S, 6.12%, Found: C, 61.77%; H, 6.47%; N, 13.20%; S, 6.00%. ^{1}H NMR: ($CDCl_3$, δ, ppm): 0.85 (t, 6H, $-CH_3$), 1.2–1.82 (m, 20H, alkyl), 4.30 (t, 4H, $-OCH_2-$), 8.10–8.31 (m, 3H, pyridine). Weight average molecular weight: 9800.

2.4. Z-scan technique

Z-scan technique, developed by Sheik Bahae et al. [13] was used to measure the third-order nonlinear optical susceptibility for our samples. In the present study, we followed the description of the experimental set-up used for our study is given briefly in Kiran et al. [11]. In the experiment, the second harmonic output of a Q-switched Nd:YAG nanosecond laser was used as the source of light. The output of the laser had a nearly Gaussian Intensity profile. The *Z*-scan data was obtained with a 50% (linear aperture transmittance ($S = 0.5$) aperture and at input intensity of 4.78×10^8 W/cm^2. To avoid cumulative thermal effects, data were collected in single shot mode [11]. Optical limiting was performed when the sample was at focal plane by varying the input laser energy and monitoring the change in the transmitted energies, simultaneously by two pyroelectric detectors with a Laser Probe Rj-7620 energy ratiometer (Laser probe Inc. Utica, NY).

3. Results and discussion

3.1. Synthesis and characterization of the polymers

The synthetic routes for the preparation of polymers **P1–P3** are shown in Scheme 1. The required precursor polyhydrazides **3a–c** were synthesized by polycondensation of 3,4-dialkoxythiophene-2,5-carbonyldihydrazides **1a–c** with pyridine 2,6-dicarbonyl chloride (**2**) in presence of anhydrous aluminium chloride and pyridine. The polyhydrazides were cyclized to the corresponding polyoxadiazoles (**P1–P3**) using phosphorus oxychloride. The formation of precursor polyhydrazides **3a–c** was evidenced by their FTIR spectral and elemental analyses. The FTIR spectrum of **3a** exhibited sharp peaks at 3220 and 1718 cm^{-1} accounting for >N–H and >C=O groups respectively. The successful conversion of polyhydrazide (**3a**) into polyoxadiazole (**P1**) was confirmed by FTIR spectrum. In its IR spectrum, disappearance of >C=O and >N–H

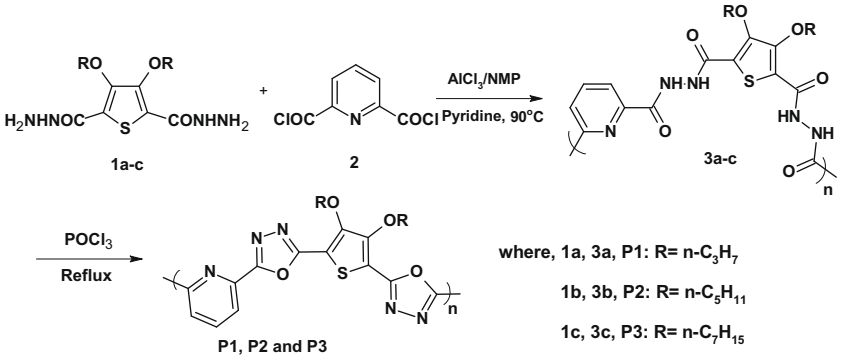

Scheme 1. Synthetic route for the preparation of copolymers.

stretching absorption bands and appearance of a sharp peak at around 1583 cm^{-1} due to imine of the oxadiazole ring indicate the cyclization. The chemical structures of these copolymers were confirmed by FTIR, ^1H NMR spectroscopy and elemental analysis. FTIR spectrum of **P1** showed characteristic absorption peaks at 2920, 2848 cm^{-1} (C–H stretching aliphatic segments), 1583 cm^{-1} (1,3,4-oxadiazole), 1467 cm^{-1} (aromatic), 1060 cm^{-1} (=C–O–C= stretching of oxadiazole). The ^1H NMR spectra of copolymer **P1** showed a multiplet at δ 8.10–8.33 ppm, due to the protons of the pyridine ring. Peaks corresponding to the protons of the alkoxy ($-OCH_2-$) groups at 3 and 4-positions of the thiophene ring appeared at δ 4.34 ppm. A set of multiplet peaks which corresponds to $-CH_2-$ appeared at δ 1.24 ppm. The methyl protons ($-CH_3$) of the alkoxy substitution resonated as a triplet at δ 0.87 ppm. The elemental analysis results of these copolymers were in agreement with their expected empirical formula. The weight average molecular weights of these copolymers, **P1, P2** and **P3** were found to be 8148, 9232 and 9800 respectively. Thermogravimetric analysis of the copolymers was carried out under nitrogen atmosphere at heating rate of 5 °C/min. The new copolymers have been found to be thermally stable up to about 300 °C. The stability of copolymers is mainly attributed to the presence of stable heteroaromatic ring systems which do not carry any active chromophores.

3.2. Electrochemical studies

Cyclic voltammetry (CV) was employed to determine redox potentials of new copolymers and then to estimate the HOMO and LUMO energy of the copolymers, which are of importance to determine the band gap. The cyclic voltammogram of the copolymer coated on a glassy carbon electrode was measured using AUTOLAB PGSTAT 30 electrochemical analyzer, using a Pt counter electrode and a Ag/AgCl reference electrode, immersed in the electrolyte [0.1 M(n-Bu)4NClO4 in acetonitrile] at a scan rate of 25 mV/s. Electrochemical data of **P1, P2** and **P3** are summarized in Table 1.

In cathodic sweep, the copolymers showed reduction peak at around −1.45 to −1.74 V. These reduction potentials are lower than those of 2-(4-*tirt*-butylphenyl)-1,3,4-oxadiazole (PBD) [14,15], one of the most widely used electron transporting materials. In the anodic sweep, copolymers showed small oxidation peak at around 2.10 V (Fig. 1), comparable with some donor acceptor type of copolymers containing 1,3,4-oxadiazole moieties reported in the literature [12]. However, the redox behaviour of these copolymers is found to be independent of length of the alkoxy side chain at 3- and 4-positions of the thiophene ring. The onset potentials of *n*- and *p*-doping processes can be used to estimate the highest occupied molecular orbital (HOMO) and lowest unoccupied molecular orbital (LUMO) energy levels of a conjugated copolymer by the equations reported by de Leeuw et al. [16],

Table 1
Electrochemical potentials and energy levels of the copolymers.

Polymer	E_{oxd}	E_{red}	E_{oxd} (onset)	E_{red} (onset)	E_{HOMO} (eV)	E_{LUMO} (eV)	E_g (eV)
P1	2.10	−1.45	1.65	−0.90	−5.98	−3.43	2.55
P2	2.08	−1.74	1.63	−0.88	−5.96	−3.45	2.51
P3	2.10	−1.51	1.70	−0.88	−6.03	−3.45	2.58

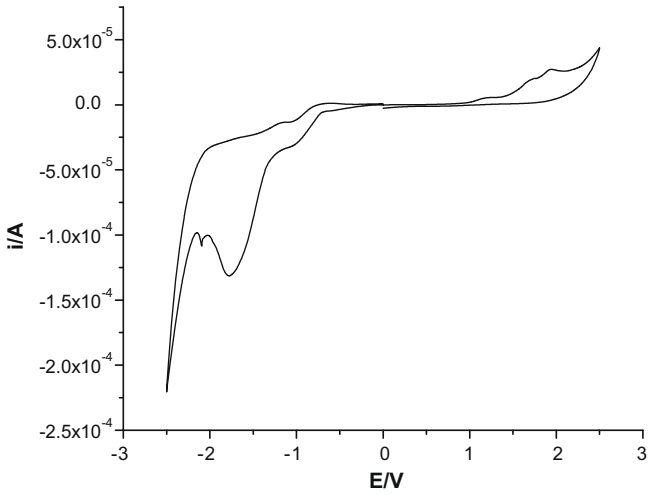

Fig. 1. Oxidation and reduction cyclic voltammetry waves of the copolymer (**P2**).

$[E_{HOMO} = -E^{oxd}_{onset} + 4.4\ eV)$ and $[E_{LUMO} = -E^{red}_{onset} + 4.4\ eV)$, where E^{oxd}_{onset} and E^{red}_{onset} are the onset potentials versus SCE for the oxidation and reduction of these copolymers. From the onset potentials of oxidation and reduction and process, the HOMO energy levels of copolymers are estimated to be at around −6.0 eV and the LUMO energy levels are found to be about −3.45 eV for all the copolymers. The band gaps of these copolymers, **P1**, **P2** and **P3** were estimated to be 2.55, 2.51 and 2.58 eV respectively.

3.3. UV–vis absorption and fluorescence emission spectroscopy

The UV–vis absorption and fluorescence spectra of the copolymers were measured in dilute DMF solutions. As shown in Fig. 2a, the absorption maxima of the copolymers, **P1**, **P2** and **P3** in dilute DMF solutions were found to be 341, 342 and 342 nm respectively. These absorption maxima were comparable to those of thiophene-1,3,4-oxadiazole copolymers [17,18]. The fluorescence emission spectra of these copolymers in solution are shown in Fig. 2b. The copolymers showed emission peaks at 469, 470 and

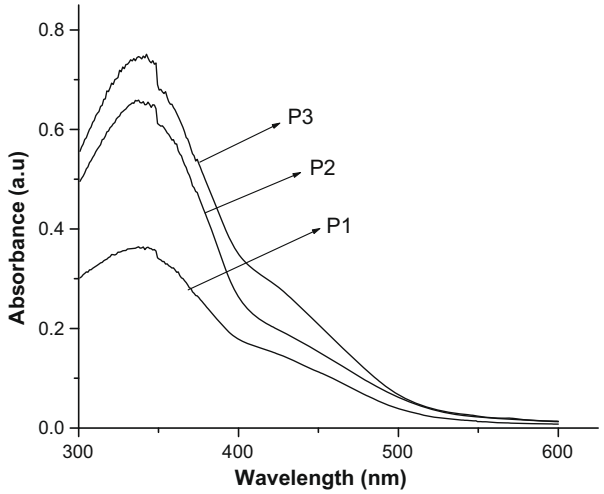

Fig. 2a. UV–visible absorption spectra of the copolymers.

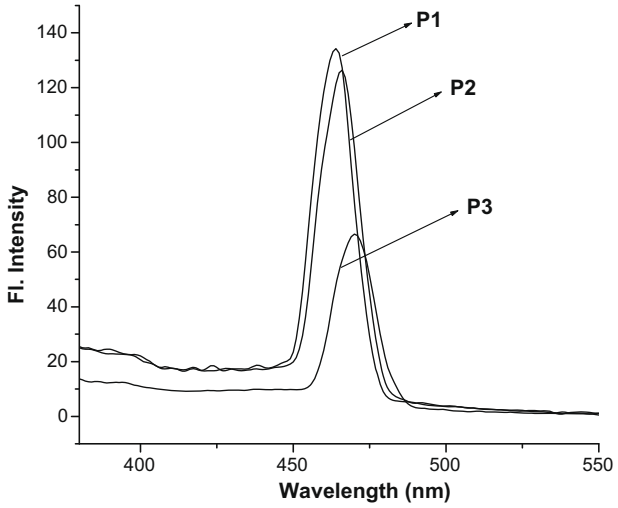

Fig. 2b. Fluorescence emission spectra of the copolymers.

470 nm for **P1**, **P2** and **P3** respectively. It has been observed that the increase in the length of the alkoxy side chain of the thiophene ring does not show significant change on the optical property. These results indicate that the copolymers emit intense bluish-green light by the irradiation of light.

3.4. Z-scan measurements

The linear absorption spectra of the copolymers in DMF solution showed that 532 nm was close to one of the absorption edges. Small absorption tails at 532 nm gives the linear absorption coefficients (α) for the copolymers, which are tabulated in the Table 2. Fig. 3 shows the open aperture *Z*-scan trace of copolymer **P2**. The transmission was symmetric about the focus [position of the sample ($Z = 0$)], where it had a minimum transmission, thus an intensity dependant absorption effect was observed. Under open-aperture *Z*-scan condition, normalized transmission is given by [19],

$$T(z) = 1 - \frac{q_o}{2\sqrt{2}} \quad \text{for} \quad |q_o| < 1 \tag{1}$$

where q_o is a free factor defined as

$$q_o = \frac{\beta I_O (1 - \exp^{-\alpha L})}{(1 + Z^2/Z_O^2)\alpha}$$

Table 2
Linear absorption coefficient, ground state absorption cross-section and excited state absorption cross-section of the copolymers.

Sample	α	σ_g ($\times 10^{-19}$ cm^2)	σ_{exc} ($\times 10^{-18}$ cm^2)
P1	0.0214	9.09	4.59
P2	0.0281	9.33	5.92
P3	0.0317	9.36	6.17

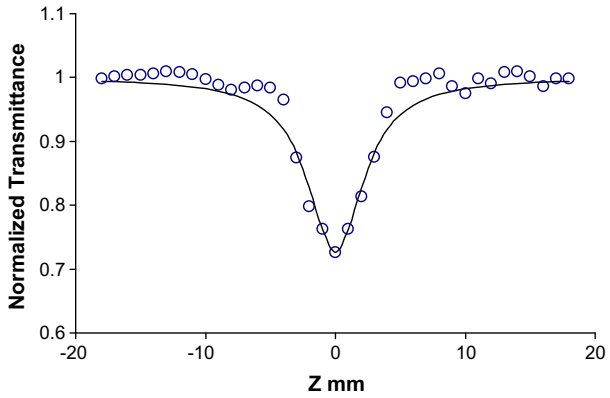

Fig. 3. Open aperture curve for **P2**. The solid line was fitted to the data from the Eq. (1) with $\beta = 16.60$ cm/GW.

where L is the length of the sample, I_o is the intensity of the laser beam at the focus, and Z_o is the Rayleigh range of the lens. A fit of the Eq. (1) to the open aperture data yielded a value of NLA of $\beta_{eff} = 16.60$ cm/GW for **P2**. The excited state absorption cross-section (σ_{ex}) was measured from the normalized open aperture *Z*-scan data [19]. It was assumed that the molecular energy levels could be reduced to a three level to calculate σ_{ex}. Molecules are optically exited from the ground state to the singlet excited state, and from this state, they relax either to ground state or to the triplet state, when exited-state absorption can occur from the triplet to the higher triplet excited state.

The change in intensity of the beam as it passes through the material is given by

$$dI/dz = \alpha I - \sigma_{ex} N(t) I \tag{2}$$

where I is the intensity, N is the number of molecules in the excited state, and t is the time. The exited-state density of the molecules appears as a result of a NLA process whose I dependence can be obtained from

$$dn/dz = \sigma_{ex} I/h\upsilon \tag{3}$$

where n is the number of molecules in the excited state, h is the plancks constant and υ is the frequency of the laser. By combining Eqs. (2) and (3) and solving for the fluence of the laser and integrating over the spatial extent of the beam, the normalized transmission T for open aperture is given as

$$T = \ln\left(1 + \frac{q_o}{1 + x^2}\right) \Big/ \frac{q_o}{1 + x^2} \tag{4}$$

where $q_o = \sigma_{ex} F_o L_{eff}/2$ hv,L_{eff} is the effective length of sample.

$$L_{eff} = (1 - \exp^{-\alpha L})/\alpha$$

A fit of Eq. (2) to the open aperture data at 532 nm with q_o yielded a value of σ_{ex} of 5.92×10^{-18} cm^2 for the polymer **P2**. The ground-state absorption cross-section (σ_g) can be calculated from

$$\alpha = \sigma_g N_a C$$

where N_a is Avogadro's number and C is the concentration (mol/cm^3). σ_g was calculated to be 9.33×10^{-19} cm^2. The value of σ_{ex} is larger than the value of σ_g, which is in agreement with the condition for observing reverse saturable absorption [19,20]. Reverse saturable absorption generally arises in a molecular system when σ_{ex} is larger than σ_g. Fig. 4 shows a plot of β_{eff} versus I_o for the copolymers in DMF. Generally, NLA can be caused by free carrier absorption, saturated absorption, direct multiphoton absorption or exited-state absorption.

If the mechanism belongs to the simple two-photon absorption, β_{eff} should be a constant that is independent of the on-axis irradiance I_o [19]. The fall off of β_{eff} with increasing I_o is a consequence of the reverse saturable absorption [21]. Therefore, we attributed this observed NLA to a reverse saturable absorption.

Fig. 5 shows the closed-aperture Z-scan trace for polymer **P2**. The pure nonlinear refraction curve, shown in Fig. 6, was obtained by the division of the closed-aperture data by the open aperture data. The Z-scan signature showed a large negative nonlinearity (self defocusing) for all the polymers. The experimental data was fitted with the following equation as described by Sheik-Bahae et al. [13]. For the closed-aperture condition the normalized transmission is given by,

$$T(z) = 1 - \frac{4\Delta\Phi_o x}{(1+x^2)(9+x^2)} \quad (5)$$

where $\Delta\Phi_o$ is the phase change and is given by

$$\Delta\Phi_o = \Delta T_{p-v}[0.406(1-S)^{0.25}]$$

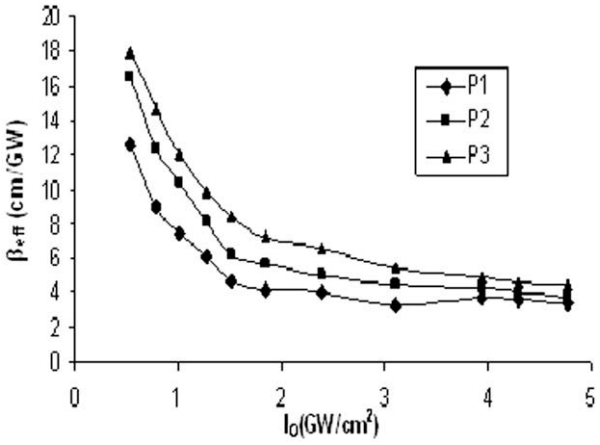

Fig. 4. Two photon absorption coefficient (β) versus in focus irradiance (I_o).

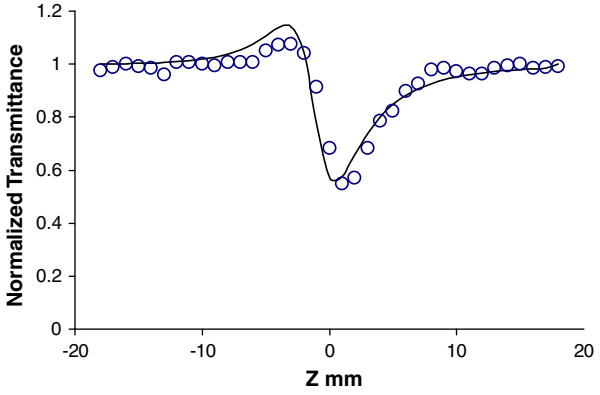

Fig. 5. Closed-apperture Z-scan curve for **P2**. Solid line depicts theoretical fit to experimental data.

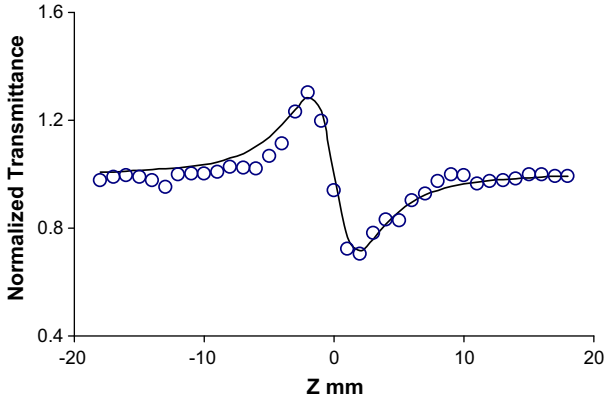

Fig. 6. Pure nonlinear absorption curve obtained through the division method for **P2**. Solid line depicts theoretical fit to experimental data.

ΔT_{p-v} is the difference between the peak and the valley of the normalized transmission. The real part of the third order nonlinear susceptibility [Re $\chi^{(3)}$] is related to n_2 and γ (m^2/W) through

$$\mathrm{Re}\chi^{(3)} = 2n_o^2 c\epsilon_o\gamma$$

where γ is nonlinear refractive index expressed in SI units, i.e. in m^2/W, n_o is linear refractive index, and c is the velocity of light. The imaginary part of the third-order nonlinear susceptibility [Im $\chi^{(3)}$] is related to the NLA through

$$[\mathrm{Im}\chi^3] = n_o^2 c\epsilon_{o\lambda}\gamma\beta_{eff}/2\pi$$

where ε_o is the permittivity of free space, and λ is laser wavelength. The nonlinear refractive index n_2 is related to γ by

$$n_2(\mathrm{esu}) = (cn_o/40\pi)x\gamma(m^2/\mathrm{W})$$

The value of n_2 is found to be of the order of 10^{-10} esu for all the three copolymers, which is nearly two orders larger then the n_2 values reported for thiophene oligomers by Hein et al. [22]. The obtained $\chi^{(3)}$ values were comparable with that obtained for poly(3-dodecyloxymethylthiophene) by Bredas and Chance [23], which is 5×10^{-12} esu. The values of third order nonlinear optical parameters (n_2 and $\chi^{(3)}$) are given in the Table 3. The copolymers contained alternating electron-donating (alkoxythiophene) and electron-withdrawing (oxadiazole and pyridine) groups in their chain and –OR refers to the alkoxy group. The length of the alkoxy groups at the 3,4-positions of the thiophene rings played an important role in the third-order nonlinear response of the copolymers. Copolymer **P3** showed a higher nonlinear response than **P1**. This may be due to higher electron-donating ability of the heptyloxy groups compared to propyloxy groups. Therefore, we attributed the enhancement in third-order nonlinear response to the increased π-electron delocalization in the copolymer.

C dependencies of NLO properties can be analysed to extract information on the NLO properties of the copolymers. C of the solutes in solution is varied, and Z-scans were repeated on solutions at each C to study the variation of nonlinear response. Fig. 7 shows the dependence of β_{eff} on **P1**, **P2** and **P3** in solution. β_{eff} varied almost linearly with the C of the sample. The NLA and NLR decreased

Table 3
Third-order nonlinear optical parameters of conjugated copolymers.

Sample	n_2 ($\times 10^{-11}$ esu)	β (cm/GW)	Re χ^3 ($\times 10^{-12}$ esu)	Im χ^3 ($\times 10^{-12}$ esu)
P1	−7.600	12.56	−0.811	0.192
P2	−8.439	16.60	−0.901	0.253
P3	−9.659	17.70	−1.030	0.272

as C in the solution decreased from 5×10^{-4} to 1.5×10^{-4} mol/L. Thus, the observed decrease in the nonlinear response was directly related to C of the samples.

3.5. Optical power limiting studies

Optical power limiting is an area of growing interest due to applications such as eye and sensor protection against intense light [24]. The nonlinear mechanisms leading to optical power limiting includes two photon absorption, free carrier absorption, reverse saturable absorption and nonlinear scattering etc. The molecules exhibiting RSA generally have extremely fast response time, since it involves electronic transitions. The best known reverse saturable absorbers are fullerene (C60), porphyrin complexes, pthalocyanines etc., [25–27]. Optical power limiting experiments was performed by keeping the cuvette containing polymer at the focus of the laser beam and measured the transmitted energy for different input laser energies. On the basis of strong reverse saturation absorption, good optical limiting properties could be expected for these copolymers. Optical limiters have been used in variety of circumstances where decrease in transmission with increase in excitation is desirable. However, one of the most important applications is eye and sensor protection in optical systems [20].

Fig. 8 demonstrates the optical limiting behaviour of **P1**, **P2** and **P3**. Among all the copolymers, the best optical limiting behaviour was observed with **P3**, which exhibited strongest NLA. For incident energies less than 20 μJ/pulse, the output linearly increased with the input. However for energies more than 20 μJ/pulse, an optical limiting of laser pulses was observed.

Fig. 9 shows the optical power limiting of the copolymer at different concentrations. The copolymer found to exhibit good optical power limiting for nanosecond laser pulses. The clamping levels of the copolymer **P2** were found to be around ~48 μJ, ~56 μJ and ~65 μJ respectively at concentrations 5×10^{-4} mol/L (**a**), 2.5×10^{-4} mol/L (**b**), 1.25×10^{-4} mol/L (**c**). The clamping levels of the copolymers decreased on increasing the concentration, this is because solutions with higher concentration posses more molecules per unit volume, hence it will absorb the laser pulses more efficiently. The alkoxy pendant substituted at the 3- and 4- position of the thiophene ring having electron, donating ability helps in enhancing optical power limiting capability of the copolymer. The thiophene based copolymers investigated here seems to be a promising candidate for making optical power limiting devices.

4. Conclusions

Three novel copolymers containing alternating 3,4-dialkoxythiophene, and (1,3,4-oxadiazolyl)pyridine moieties have been synthesized and characterized. The new copolymers have well defined structure and good thermal stability. They show bluish-green fluorescence under the irradiation of UV light. Cyclic voltammetry studies reveal that these copolymers have low-lying LUMO (−3.43 to −3.45 eV) energy levels and high-lying HOMO (−5.96 to −6.03 eV) energy levels. The third-order NLO measurements obtained from the single beam Z-scan technique showed that the copolymers possess high $\chi^{(3)}$ values, that were comparable with those reported for poly(3-dodecyloxymethylthiophene) and poly(*p*-phenylenevinylene) copolymers. The dependence of NLO parameters on the length of the alkoxy substituents present in the copolymers indicated the electronic origin of nonlinearity. All the copolymers showed strong reverse saturation absorption and good optical limiting properties at 532 nm. Hence, these copolymers can be used for the optical power limiting application.

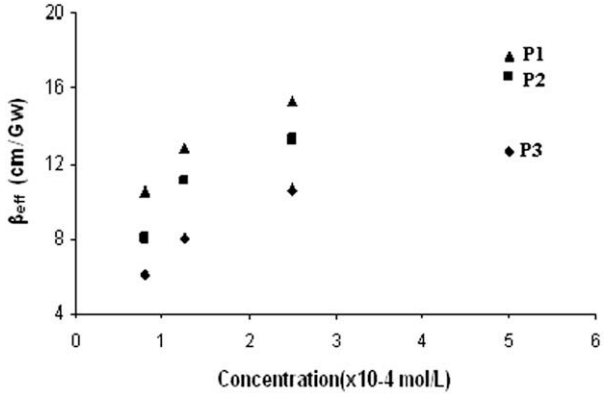

Fig. 7. Concentration dependence of absorption coefficient (β) for the copolymers.

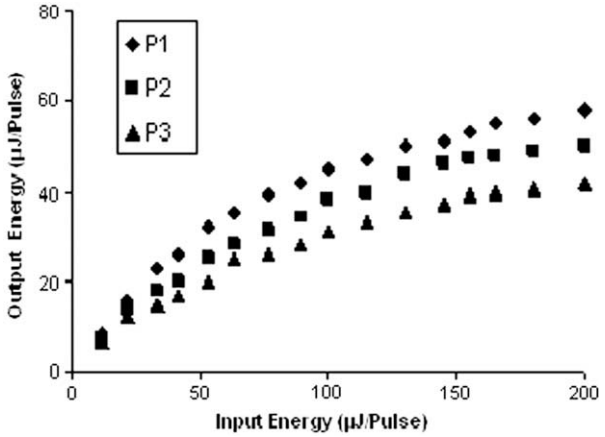

Fig. 8. Optical limiting behaviour of the copolymers **P1**, **P2** and **P3**.

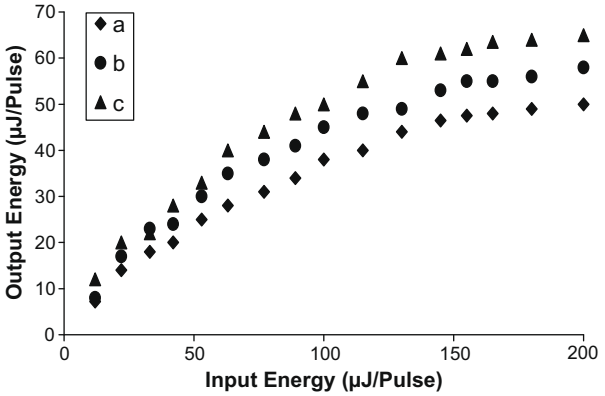

Fig. 9. Optical limiting behaviour of polymer **P2** at different concentration.

Acknowledgements

The authors are grateful to the CDRI, Lucknow, NMR research centre, IISc Bangalore and RRL, Trivandrum, for providing instrumental analyses.

References

[1] L.H. Hornak, Polymers for Light Wave and Integrated Optics, Marcel Dekker, New York, 1992.
[2] R.W. Munn, C.N. Ironside (Eds.), Principles and Applications of Nonlinear Optical Materials, Chapman and Hall, London, 1993.
[3] T. Cassano, R. Tommasi, M. Ferrara, F. Babudri, G.M. Farinola, F. Naso, Chem. Phys. 272 (2001) 111.

[4] P.N. Prasad, D.J. Williams, Introduction to Nonlinear Optical Effects in Molecules and Polymers, Wiley, New York, 1992.
[5] E.V. Keuren, T. Wakebe, R. Andreaus, H. Mohwald, W. Schrof, V. Belov, H. Matsuda, R. Rangel-Rojo, Appl. Phys. Lett. 75 (1999) 3312.
[6] M. Nisoli, A. Cybo-Ottone, S. De Silvestri, V. Magni, R. Tubino, C. Botta, A. Musco, Phys. Rev. B 47 (1993) 10881.
[7] S. Kishino, Y. Ueno, K. Ochiai, M. Rikukawa, K. Sanui, T. Kobayashi, H. Kunugita, K. Ema, Phys. Rev. B 54 (1998) 430.
[8] I. Fuks-Janczarek, I.V. Kityk, R. Miedzinski, E. Gondek, A. Danel, M. Zagorska, Spectrochemica Acta: Part A 64 (2006) 264.
[9] D. Udayakumar, A. John Kiran, A.V. Adhikari, K. Chandrasekharan, H.D. Shashikala, J. Appl. Poly. Sci. 106 (2007) 3033.
[10] D. Udayakumar, A. John Kiran, A. Vasudeva Adhikari, K. Chandrasekharan, G. Umesh, H.D. Shashikala, Chem. Phys. 331 (2006) 125.
[11] J.A. Kiran, K. Chandrashkaran, R.N. Satheesh, H.D. Shashikala, G. Umesh, B. Kalluraya, Chem. Phys. 324 (2006) 699.
[12] D. Udayakumar, A.V. Adhikari, Synth. Met. 156 (2006) 1168.
[13] S.M. Bahae, A. Said, T.H. Wei, D.J. Hagan, E.W. Vanstryland, IEEE J. Quant. Electr. 26 (1990) 760.
[14] M. Strukelj, F. Papadimitrakopoulos, T.M. Miller, L.J. Rothberg, Science 267 (1995) 1969.
[15] S. Janietz, A. Wedel, R. Friedrich, Synth. Met. 84 (1997) 381.
[16] D.M. de Leeuw, M.M.J. Simenon, A.B. Brown, R.E.F. Einerhand, Synth. Met. 84 (1997) 53.
[17] W.L. Yu, H. Meng, J. Pei, W. Huang, Y. Li, A.J. Heeger, Macromolecules 31 (1998) 4838.
[18] W. Huang, H. Meng, J. Pei, Z. Chen, Y. Lai, Macromolecules 32 (1999) 118.
[19] F.Z. Henari, W.J. Blau, H.R. Milgrom, G. Yashigolu, D. Philips, J.A. Lacey, Chem. Phys. Lett. 267 (1997) 229.
[20] L.W. Tutt, T.F. Boggess, Prog. Quant. Electron. 17 (1993) 299.
[21] S.-L. Guo, L. Xu, T.H. Wang, X.Z. You, N.B. Ming, Optik 114 (2003) 58.
[22] J. Hein, H. Bergner, M. Lanzner, S. Rantsch, Chem. Phys. 179 (1994) 543.
[23] J.L. Bredas, R.R. Chance (Eds.), Conjugated Polymeric Materials: Opportunities in Electronics, Optoelectronics, and Molecular Electronics, Kluwer Academic, Boston, 1989, p. 399.
[24] J.W. Perry, K. Mansour, I.-Y.S. Lee, X.-L. Wu, P.V. Bedworth, C.-T. Chen, D. Ng, S.R. Marder, P. Miles, T. Wada, M. Tian, H. Sasabe, Science 273 (1996) 1533.
[25] L. Richard, Sutherland, Handbook of Nonlinear Optics, Dekker, New York, 1996.
[26] Jean Roncali, Chem. Rev. 92 (1992) 711.
[27] T. Cassano, R. Tommasi, F. Babudri, A. Cardone, G.M. Farinola, F. Naso, Optics Lett. 27 (2002) 2176.